ISSN: 1813-4890

Research on Mechanical Properties of Hydrate-Bearing Sediments Based on Numerical Simulation

Fu Su, Jianqiang Han

North China University of Science and Technology, Tangshan 063210, China

Abstract

Based on experimental findings for hydrate-bearing sediments (HBS), this study employs the Abaqus finite element analysis software and utilizes the UHARD subroutine to define a user-customized constitutive model. It investigates the impact of hydrate occurrence on the mechanical properties of sediments, such as elastic modulus and shear strength. A numerical model for the mechanical behavior of HBS was developed based on finite element theory, and numerical simulations were conducted under the influence of multiple factors, including varying NaCl concentration, temperature, hydrate saturation, and effective confining pressure. The numerical simulation results were compared and analyzed against triaxial test data, revealing a model error range between 0.9% and 6.5%, which validates the accuracy and reasonableness of the numerical model. The study finds that the relationship between yield strength and temperature is nonlinear, indicating that reservoir subsidence should be prioritized during the extraction process. Additionally, hydrate saturation significantly affects the mechanical properties, highlighting the necessity of closely monitoring hydrate dissociation during extraction.

Keywords

Hydrate-Bearing Sediments; Numerical Simulation; Mechanical Properties Study; UHARD.

1. Introduction

The extraction of natural gas from marine domains is a complex multi-field coupling process influenced by multiple factors. This process can lead to the degradation of hydrate-bearing sediment (HBS) reservoirs, triggering a series of marine geotechnical disasters such as continental shelf landslides and seabed collapse, further causing economic losses[1]. Therefore, to ensure the safe and economical extraction of marine natural gas, fully understanding the deformation laws of HBS is essential[2]. Finite element analysis (FEA) is one of the effective approaches to study the properties of HBS, especially when experimental techniques and conditions are limiting, highlighting the advantages of FEA. However, in FEA, efficient modeling methods and reasonable material constitutive models are required to ensure the accuracy of the results[3].

Currently, numerical simulation research on HBS is gradually being refined. Researchers are progressively introducing parameters such as saturation, cementation, and damage into numerical models, but the complexity of obtaining and solving these parameters increases accordingly[4]. Therefore, using the stress-strain relationship obtained from laboratory tests as an elasto-plastic constitutive model for numerical simulation not only simplifies the simulation process but also holds significant research value.

This paper integrates the elasto-plastic constitutive model for HBS with experimental conclusions, develops finite element programs, constructs a numerical model for HBS based on finite element theory, performs numerical simulations of some laboratory tests, realizes

ISSN: 1813-4890

numerical simulation of the evolution of mechanical properties of HBS under thermo-mechanical-chemical (TMC) multi-field coupling conditions, builds a numerical model that can reflect the evolution laws of mechanical properties of HBS under varying multi-factor conditions, compares numerical simulation results with experimental data to validate the model's reasonableness, conducts supplementary simulation tests to provide reasonable suggestions for HBS extraction, and engages in extended discussion.

2. Introduction to ABAQUS and Its Secondary Development

2.1. Introduction to ABAQUS

ABAQUS, as a world-class finite element analysis platform, holds a core position in multi-physics interaction analysis due to its exceptional numerical solution accuracy and highly modular secondary development environment. This research delves into the mechanical behavior of HBS under complex environments, and ABAQUS is the key tool for achieving this goal. Its core solver is written in Fortran, capable of efficiently resolving complex nonlinear, multi-field coupling problems under a large-scale parallel computing framework. Meanwhile, its pre- and post-processing modules are built on Python, providing a flexible and powerful environment for automated modeling, data processing, and user-defined interfaces[5].

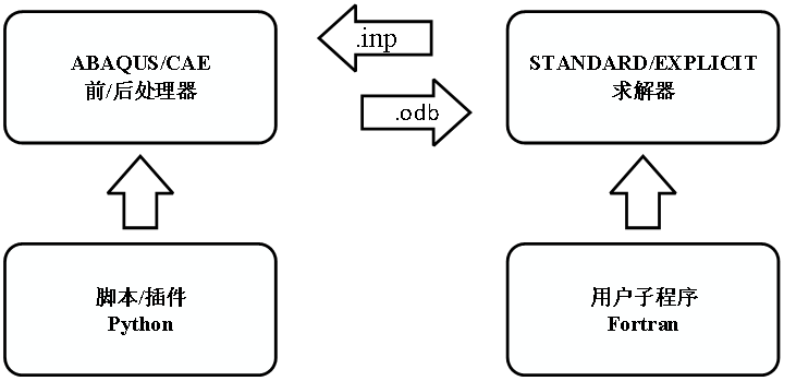

Fig.1 ABAQUS Software Structure

The user subroutine interface of ABAQUS provides a solid platform for the innovative methods of this study. Through this interface, we seamlessly embedded our self-developed UHARD subroutine into the ABAQUS solution process, achieving real-time monitoring and precise updating of the nonlinear hardening behavior of HBS materials[6]. This close integration not only breaks through the limitations of traditional single-factor models in describing multi-field coupling effects but also provides strong numerical support for the dynamic response to environmental factors such as temperature, NaCl concentration, and hydrate saturation. The system architecture shown in Figure 1 illustrates the specific application flow of ABAQUS in the pre-processing, solving, and post-processing stages of this study, fully demonstrating its adaptability and extensibility in solving complex engineering problems.

2.2. Principles of the UHARD Subroutine

In the high-precision simulation of the mechanical behavior of HBS, accurately capturing the nonlinear transition of the material from elastic response to plastic evolution has always been the key to solving multi-field coupling problems. For this purpose, this study innovatively developed a custom hardening subroutine, UHARD, based on the J2 plastic flow theory[7]. Its design concept is to seamlessly embed multiple environmental factors such as temperature, NaCl concentration, and hydrate saturation into the elasto-plastic constitutive model, achieving real-time updates of the material yield state and hardening parameters to faithfully reproduce the dynamic response of sediments under complex working conditions.

ISSN: 1813-4890

The UHARD subroutine employs an advanced incremental plasticity algorithm: within each loading increment, the system first comprehensively considers the current strain state and external environmental parameters to accurately calculate the initial yield intercept and hardening modulus; subsequently, it performs plastic correction on the trial stress through strict consistency conditions and a radial return algorithm, constructing a tangent stiffness matrix highly compatible with the incremental plastic process, thus ensuring a smooth transition of the material from the elastic to the plastic zone and the stability of the numerical solution[8].

Within the ABAQUS platform, UHARD, as a custom constitutive module, is deeply integrated with the core solver through the user subroutine interface, achieving real-time response and dynamic updating of material behavior under multi-field coupling conditions. This innovative method not only breaks through the limitations of single-factor constitutive models in describing environmental coupling effects but also provides cutting-edge technical support for the high-precision simulation of the mechanical properties of HBS. Validation against extensive triaxial test data shows its excellent performance in capturing complex nonlinear responses and multi-physicochemical field coupling effects, offering new ideas for solving future cross-scale, multi-physicochemical field coupling problems.

3. The Construction Process of Numerical Models for Hydrate-Bearing Sediments

3.1. Confirmation of Related Parameters and Model Assumptions for Elasto-Plastic Linear Hardening

Based on the stress-strain law of hydrate-bearing sediments obtained from laboratory tests in the paper by Jin[9] et al., this section shows that the constitutive behavior of hydrate-bearing sediments is elastoplastic. Regarding the evolution law of elastoplasticity, it can be mainly divided into the following four types: a) ideal elastoplasticity, b) ideal rigid-plasticity, c) elastoplastic linear hardening, and d) rigid-plastic linear hardening[10]. The yield law obtained from the tests is similar to c) elastoplastic linear hardening. Therefore, the derivation is carried out based on the elastoplastic linear hardening constitutive model, and the relevant parameters required for simulation are determined according to the laboratory tests in the paper by Jin[9] et al., so as to realize the numerical simulation of hydrate-bearing sediments under multi-field coupling conditions.

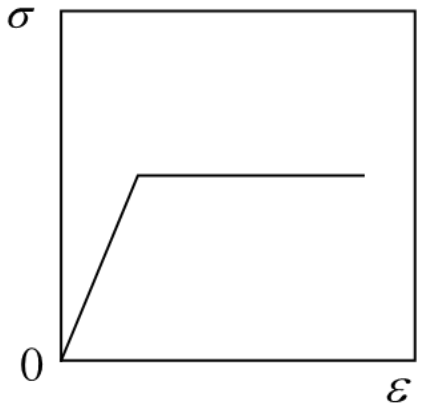

(a)Ideal Elastic-Plastic Constitutive Model

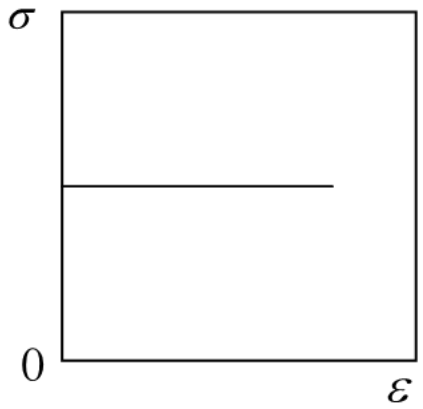

(b)Ideal Rigid-Plastic Constitutive Model

ISSN: 1813-4890

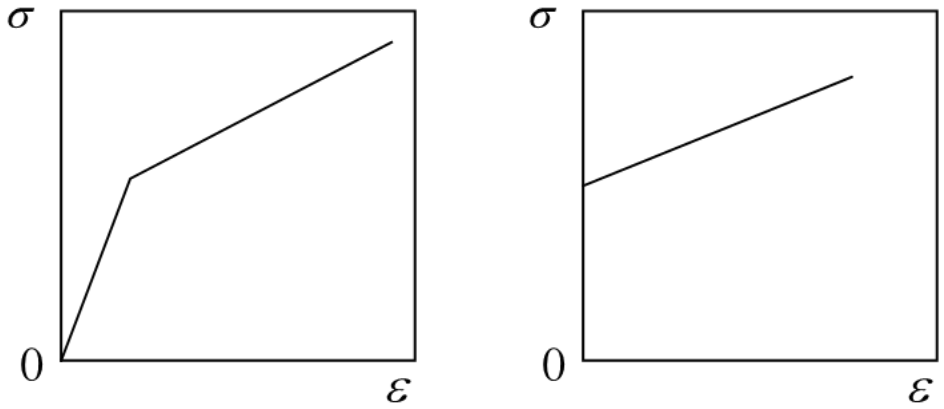

(c)Elastoplastic Linear Hardening Constitutive Model (d)Rigid-Plastic Linear Hardening Constitutive Model

Fig.2 Different Yield Criteria

For the elastoplastic linear hardening constitutive model, it mainly consists of a linear elastic region and a linear plastic region [11]. The constitutive relationship is divided into an elastic part and a plastic part for independent calculation. This method simplifies the calculation of the constitutive model; it is only necessary to determine the yield strength, elastic modulus, and hardening modulus to establish the elastoplastic linear hardening constitutive relationship.

$$\begin{cases} \sigma = E\grave{o}_e \\ \sigma = \sigma_0 + H\grave{o}_p \\ \varepsilon = \varepsilon_e + \varepsilon_p \end{cases} \tag{1}$$

Wherein: σ : Stress;

E : Elastic modulus;

$\grave{o}_e$: Elastic strain;

σ_0 : Yield strength;

H : Hardening modulus;

ε_p : Plastic strain.

All the above parameters can be obtained from the indoor triaxial shear tests in the paper by Jin[9] et al., and several groups of supplementary experiments under different temperatures have been conducted. The influence of different coupling conditions (TMC) on hydrate-bearing sediments during the tests is converted into the influence on mechanical parameters, and empirical formulas are derived to reflect the relationships between hydrate saturation, temperature, NaCl concentration and various mechanical parameters. Test data were collected under the conditions of 8 MPa confining pressure with different NaCl concentrations, as well as different saturations and different temperatures. Regression analysis was performed on these parameters to obtain the relationships between different parameters and environmental factors, and the regression analysis diagrams are shown below:

ISSN: 1813-4890

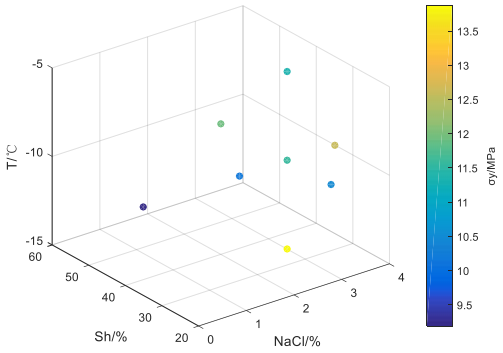

Fig.3 Regression Analysis of Yield Strength

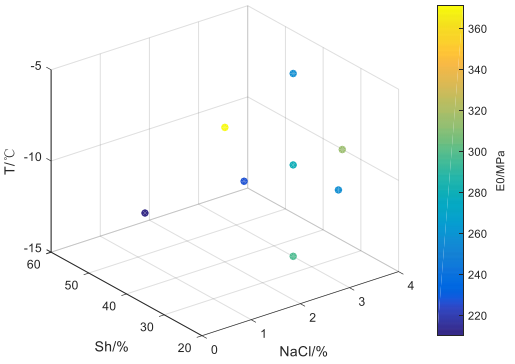

Fig.4 Regression Analysis of Elastic Modulus

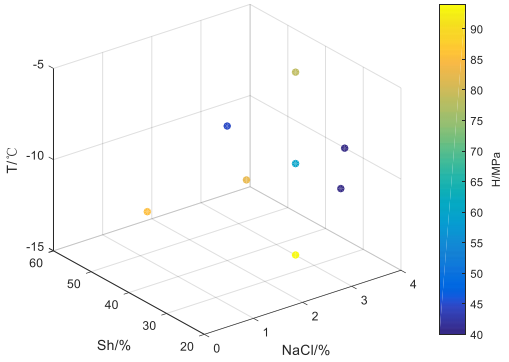

Fig.5 Regression Analysis of Hardening Modulus

Empirical formulas between different parameters and various factors were obtained through fitting, with expressions as follows:

$$\sigma_0 = 5.038 + 0.9011M_s + 0.0415S_h - 0.251T \tag{2}$$

$$H = 79.597 - 10.22M_s - 0.088S_h - 1.6T \tag{3}$$

$$E_0 = 18.474 + 28.131M_s + 4.037S_h - 4T \tag{4}$$

Where: M_s : NaCl concentration;

S_h : Hydrate saturation;

T : Environmental temperature.

Among them, the elastic modulus is used to construct the constitutive stiffness matrix, and combined with Poisson's ratio (selected based on experiments), the shear modulus and bulk modulus are obtained. Based on the isotropic hardening model, incremental plasticity theory is adopted, and it is assumed that the material satisfies the Mises yield surface accompanied by the flow rule, i.e., the J2 (Mises) yield criterion is used. Then the yield function can be written as [12]:

$$f(\sigma, \bar{\varepsilon}^p) = \sigma_{eq}(\sigma) - \left[\sigma_0 + H\bar{\varepsilon}^p\right] = 0 \tag{5}$$

$$\sigma_{eq}(\sigma) = \sqrt{\frac{3}{2}\sigma^{dev} : \sigma^{dev}} \tag{6}$$

Where: $f(\sigma, \bar{\varepsilon}^p)$: The yield function of the material, which defines the yield condition of the material. When $f < 0$, the material is in an elastic state, and no plastic deformation occurs; when $f = 0$,the material just reaches the yield state; when $f > 0$, the material has exceeded the yield, and plastic correction should be performed.

$\bar{\varepsilon}^p$: Cumulative equivalent plastic strain;

ISSN: 1813-4890

$\sigma_{eq}(\sigma)$: Von Mises equivalent stress;

σ^{dev}: Deviatoric stress of the stress tensor.

3.2. Implementation of the UHARD Subroutine

In Abaqus, the UHARD subroutine has two primary tasks. First, it returns the yield stress and the derivative with respect to the equivalent plastic strain based on the current equivalent plastic strain, temperature, and field variables (such as NaCl concentration and hydrate saturation). Second, Abaqus internally combines the built-in Mises yield surface and incremental plasticity algorithm to perform stress update and stiffness matrix calculation. The pseudo-code for the example calculation is shown in the figure.

```
Algorithm  User Hardening Subroutine (UHARD)
1:  procedure UHARD(SYIELD, H, EQPLAS, EQPLASRT, TEMP, DTIME, CMNAME, NSTATV, STATEV)
2:      Initialization:
3:          Read state variables: T ← STATEV(1), Sh ← STATEV(2), Ms ← STATEV(3)
4:      Compute sigma0 and HMOD:
5:          sigma0 ← 5.038 + 0.9011 * Ms + 0.0415 * Sh - 0.251 * T
6:          HMOD ← 79.597 - 10.22 * Ms - 0.0885 * Sh - 1.60 * T
7:      Compute yield stress:
8:          SYIELD ← sigma0 + HMOD * EQPLAS
9:      Return hardening modulus:
10:         H ← HMOD
11:     Update state variables:
12:         STATEV(1) ← T, STATEV(2) ← Sh, STATEV(3) ← Ms
13:     return
14: end procedure
```

Fig.6 Pseudo-Code of the UHARD Subroutine

3.3. Modeling Process of the Numerical Model

In this study, a numerical model of hydrate-bearing sediments was established on the ABAQUS platform, and the modeling process started with geometric modeling, material property definition, and constitutive interface integration. Firstly, a geometric model with the same dimensions was constructed based on the model size and key parameters of the laboratory experiment described in the paper by Jin [9] et al., and the material parameters obtained from the experiment were imported using a Python script. Through the user subroutine interface, the independently developed UHARD subroutine was embedded into the ABAQUS solution process to realize the dynamic update of the elastoplastic linear hardening constitutive relation. This enabled the real-time reflection of multi-field coupling effects (such as temperature, NaCl concentration, and hydrate saturation) in the material behavior, thereby breaking through the limitations of traditional single-factor models.

After the model assembly was completed, the corresponding loads and boundary conditions were applied in accordance with the experimental loading scheme, and the sweeping method was used for mesh generation to balance calculation accuracy and efficiency. The element type adopted for the hydrate reservoir was the C3D8P element, which can simulate the pore fluid flow and solid deformation during the experiment, and the total number of C3D8P elements was 9900. Finally, the compiled Fortran UHARD subroutine was called through the ABAQUS job module to realize the real-time update of material constitutive parameters during the numerical solution process. In the post-processing stage, stress-strain data were extracted, and the model accuracy was verified by comparing with the experimental results. This in-depth integration of ABAQUS and the UHARD subroutine not only greatly simplifies the constitutive solution process under complex multi-field coupling but also provides an efficient and accurate numerical simulation tool for engineering applications.

ISSN: 1813-4890

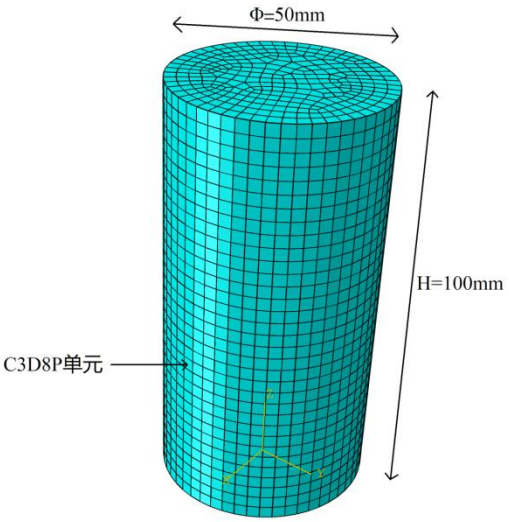

Fig.7 Schematic Diagram of the Numerical Simulation Model for Hydrate-Bearing Sediments

4. Verification of the Numerical Simulation of Hydrate-Bearing Sediments Under Multi-Field Coupling

In this section, the numerical simulation results obtained from the established model were compared with the indoor experimental data from Jin's [9] paper and several supplementary experiments. Through comparisons under different NaCl concentrations, different confining pressures, different temperatures, and different hydrate saturations, error analysis of the established numerical model was conducted, and in-depth discussions were carried out. The specific simulation schemes are detailed in Table 1.

Table 1. Simulation Schemes

NO.	NaCl/%	Temperature/℃	Saturation/%	Confining Pressure/MPa
S1	0	-10	35	8
S2	2	-10	35	8
S3	3	-10	35	8
S4	4	-10	35	8
S5	3	-10	35	5
S6	3	-10	35	10
S7	3	-10	24	8
S8	3	-10	53	8
S9	3	-5	35	8
S10	3	-15	35	8

4.1. Comparison Between Numerical Simulation and Test Data Under Different NaCl Concentrations

The triaxial compression test data of hydrate-bearing sediments under different NaCl concentrations were compared with the numerical simulation results under the same conditions.

ISSN: 1813-4890

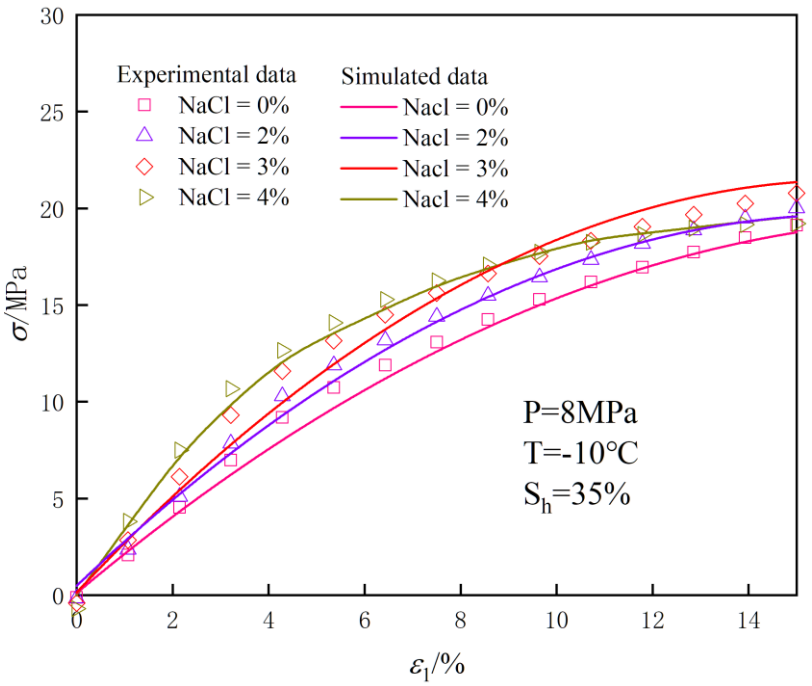

Fig.8 Comparison Between Indoor Tests and Numerical Simulations Under Different NaCl Concentrations

From the data comparison in Figure 8, it can be seen that under the same environmental conditions, the numerical simulation results of hydrate-bearing sediments under different NaCl concentrations are in good agreement with the triaxial compression test data in both the elastic stage and the plastic stage, and the yield strength and shear strength are also relatively consistent.

When the NaCl concentration is 0%, the test data and numerical data in the elastic stage are in good agreement; when entering the plastic stage, a small deviation occurs between the test data and numerical data, which may be because the model does not fully capture the softening characteristics under low-salt conditions, but this does not affect the simulation effect. When the NaCl concentration is 2%, the test data and numerical data in the elastic stage are also in good agreement, but a small deviation occurs during the transition to the plastic stage, and this deviation gradually disappears with the development of plastic strain, having a small impact on the data. When the NaCl concentrations are 3% and 4%, the laws reflected by the test data and numerical data are consistent with those at a NaCl concentration of 2%: a deviation occurs during the transition from the elastic stage to the plastic stage, and then the deviation gradually decreases with the increase of plastic strain. This may be due to the overestimation of plastic hardening by the model, indicating that the model still has room for optimization in terms of plastic effects under high-salt environments. However, the overall trend is consistent, and the overall error is small. The analysis shows that the numerical model can well reflect the mechanical properties and evolution laws of hydrate-bearing sediments under different NaCl concentration gradients.

4.2. Comparison Between Test Data and Numerical Simulation Under Different Confining Pressures

The triaxial compression test data of hydrate-bearing sediments under different confining pressures were compared with the numerical simulation results under the same conditions.

ISSN: 1813-4890

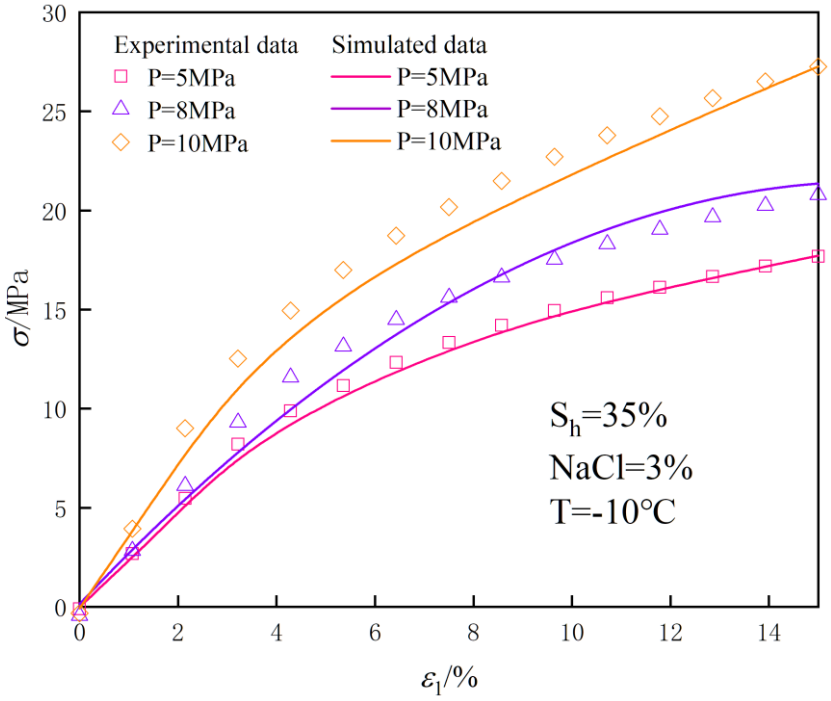

Fig.9 Comparison Between Indoor Tests and Numerical Simulations Under Different Confining Pressures

From the data comparison in Figure 9, it can be seen that under the same environmental conditions, the numerical simulation results of hydrate-bearing sediments under different confining pressures are in good agreement with the triaxial compression test data in both the elastic stage and the plastic stage, and the yield strength and shear strength are also relatively consistent.

When the confining pressure is 5 MPa, the test data and numerical simulation data are basically consistent in the elastic stage, indicating that the model can well describe the initial loading characteristics of hydrate-bearing sediments. However, when entering the plastic stage, a small deviation occurs between the test data and numerical data, which may be due to the model's insufficient capture of the softening effect, leading to a slight underestimation or overestimation of the simulation data. Nevertheless, the overall trend remains consistent, and the impact on the simulation effect is small. When the confining pressure increases to 8 MPa and 10 MPa, the deviation between the test data and simulation data decreases, and the matching degree in the elastic stage remains high. However, in the plastic stage, the numerical simulation results are slightly higher than the test data, which may be due to the model's overestimation of the plastic hardening effect. This indicates that although the numerical model can well reflect the stress-strain relationship of hydrate-bearing sediments under higher confining pressures, further optimization is still needed in the plastic stage to more accurately capture the softening characteristics.

Overall, the numerical model can accurately simulate the mechanical response of hydrate-bearing sediments under different confining pressures, showing good fitting effects in both the elastic stage and the plastic stage, with small errors in yield strength and shear strength and consistent overall trends. Thus, it can be used for further research on the influence of confining pressure on the mechanical properties of hydrate-bearing sediments.

4.3. Comparison Between Test Data and Numerical Simulation Under Different Hydrate Saturations

The triaxial compression test data of hydrate-bearing sediments under different hydrate saturations were compared with the numerical simulation results under the same conditions.

ISSN: 1813-4890

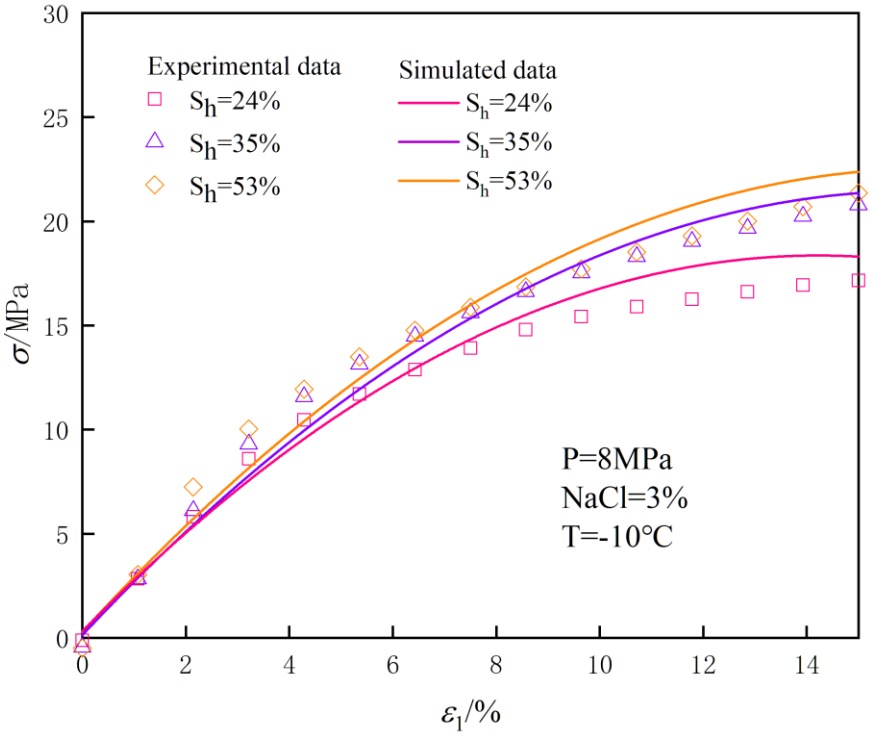

Fig.10 Comparison Between Indoor Tests and Numerical Simulations Under Different S_h Conditions

From the data comparison in Figure 10, it can be seen that under the same environmental conditions, the numerical simulation results of hydrate-bearing sediments under different hydrate saturations are in good agreement with the triaxial compression test data in both the elastic stage and the plastic stage, and the yield strength and shear strength are also relatively consistent.

When the saturation S_h = 24%, the test data and numerical data in the elastic stage are in good agreement. Since the transition from the elastic stage to the plastic stage is smoother than the data in the previous two sections, there is no obvious error between the test data and numerical data in the transition stage. However, the test curve in the plastic stage is also non-linear, which may be because the model does not fully capture the microstructural changes under low hydrate content, resulting in a small error between the numerical data and test data in the plastic stage. When the saturation $S_h \geq 35\%$, the test data and numerical data in both the elastic stage and the plastic stage are in good agreement. It can be seen that when the saturation exceeds the critical value of 35%, the influence of saturation on the stress-strain curve is small but still exists. However, the difference between the numerical data is small because the numerical data tend to be linear during the iteration process. The analysis shows that the numerical model can well reflect the mechanical properties and evolution laws of hydrate-bearing sediments under different hydrate saturation conditions, with a high overall matching degree.

4.4. Comparison Between Test Data and Numerical Simulation Under Different Temperatures

The triaxial compression test data of hydrate-bearing sediments under different temperatures were compared with the numerical simulation results under the same conditions.

ISSN: 1813-4890

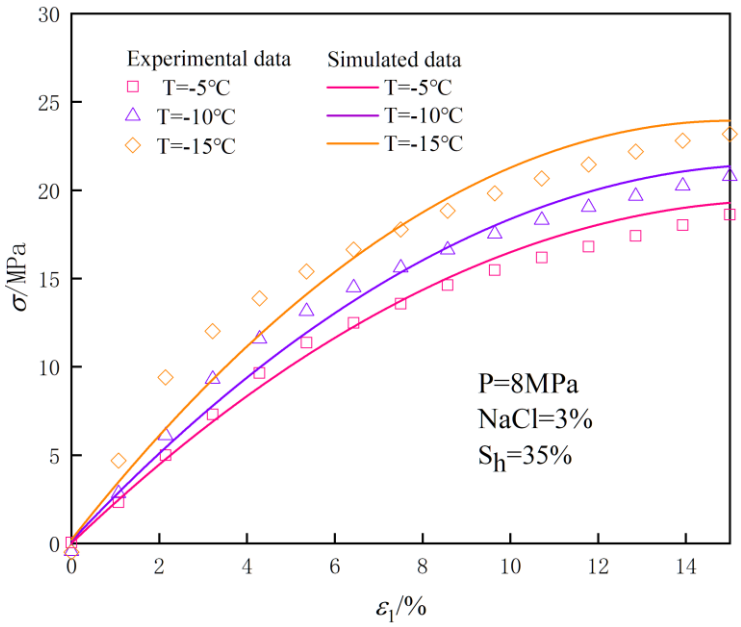

Fig.11 Comparison Between Indoor Tests and Numerical Simulations Under Different Temperatures

From the data comparison in Figure 11, it can be seen that under the same environmental conditions, the numerical simulation results of hydrate-bearing sediments under different temperatures are in good agreement with the triaxial compression test data in both the elastic stage and the plastic stage, and the yield strength and shear strength are also relatively consistent.

When the temperature is -5°C, the test data and numerical simulation data are basically consistent in the elastic stage, indicating that the model can well describe the initial loading characteristics of hydrate-bearing sediments at relatively high temperatures (corresponding to a relatively low freezing degree). However, in the plastic stage, the numerical simulation data are slightly higher than the test data, which may be due to the model's deviation in capturing the softening effect at higher temperatures. When the temperature decreases to -10°C and -15°C, the deviation between the test data and simulation data gradually decreases, and the fitting degree in the elastic stage is relatively high. However, in the plastic stage, as the temperature decreases, the stress values of the numerical simulation results are slightly higher than the test data, which may be due to the model's overestimation of the plastic hardening effect under low-temperature conditions, leading to the simulation data being slightly higher than the test data.

From the overall trend, a decrease in temperature enhances the bearing capacity of hydrate-bearing sediments. That is, at lower temperatures (-15°C), the yield strength and shear strength are higher, showing stronger deformation resistance, which is consistent with the overall trend of the test data. Therefore, the numerical model can accurately reflect the evolution laws of the mechanical properties of hydrate-bearing sediments under different temperature conditions, but there is still room for optimization in the plastic stage under low temperatures to further improve the simulation accuracy.

4.5. Error Analysis of the Numerical Model

The yield strength and shear strength from the stress-strain curves of the numerical simulation were compared with those from the tests, and a quantitative analysis was conducted to evaluate the numerical model. Table 2 shows the errors between the 10 groups of numerical simulations and the tests. It can be seen from Table 2 that the maximum error of the numerical model

ISSN: 1813-4890

constructed in this study is 6.5%, and the minimum error is 0.9%, which is within the standard error range, indicating the rationality of the numerical model.

Table 2. Errors of the Numerical Simulation

NO.	Yield Strength Error	Shear Strength Error
S1	2.7%	1.9%
S2	1.5%	2.1%
S3	1.8%	2.7%
S4	3.5%	2%
S5	6.5%	0.9%
S6	6.4%	1.1%
S7	3.2%	6.3%
S8	3.1%	4.8%
S9	1.1%	3.6%
S10	0.9%	3.3%

By analyzing the errors of the numerical simulation, it was found that the slope of the curve is continuously updated during the iteration process of the model. For parts with strong non-linearity, slight errors may occur. For example, in Groups 1, 2, 3, 4, 8, 9, and 10, the errors of yield strength and shear strength are all around 1% - 4%. There is neither an extremely high single-item error nor an obvious large deviation, indicating that the non-linearity of these specimens in the elastoplastic transition and final failure stages is not extreme, and the numerical model has good adaptability to them.

For Groups 5 and 6, due to the influence of variables, the test stress-strain curves have a high yield strength error but a very low shear strength error. This may be because the slope changes sharply during the transition from the elastic stage to the plastic stage, and the material or boundary conditions are sensitive to the prediction of the yield point; however, the later failure stage is relatively easy to fit. On the contrary, Group 7 has a moderate yield strength error but a significantly higher shear strength error. This may be because the model can reasonably capture the yield point of this specimen, but local stress concentration or crack propagation may occur in the final failure stage, leading to a large deviation. In general, these specimens show unbalanced simulation accuracy in the "early and late stages". In the future, the material constitutive model and iteration algorithm in the yield zone or failure zone can be improved in a targeted manner.

Overall, this set of data shows that the numerical model can well reproduce the experimental results for most specimens, demonstrating a certain degree of reliability, but there is still room for improvement.

5. Analysis of the Influence of Exploitation on the Mechanical Properties of Hydrate-Bearing Sediments

The current basic idea for hydrate exploitation is to destroy the phase equilibrium state of hydrate-bearing sediments and promote their dissociation. However, this process will inevitably affect the performance of hydrate-bearing sediment reservoirs. Therefore, it is necessary to analyze the influence of exploitation on the mechanical properties of hydrate-bearing sediments [13]. The above verification proves that the model can define the constitutive relationship of hydrate-bearing sediments under different environmental conditions and can well reflect the mechanical properties of hydrate-bearing sediments under such conditions. Therefore, temperatures above 0°C and gradually decreasing hydrate saturation were set to

ISSN: 1813-4890

simulate the effect of temperature-induced dissociation. The supplementary simulation tests are shown in Table 3.

Table 3. Numerical Simulation of Hydrate-Bearing Sediment Exploitation

No.	NaCl/%	Temperature/°C	Saturation/%	Confining Pressure/MPa
S1	3	0	35	8
S2	3	1	35	8
S3	3	3	35	8
S4	3	5	35	8
S5	3	5	15	8
S6	3	5	0	8

The supplementary simulation data were analyzed to discuss the influence of temperature increase (including hydrate dissociation) on the mechanical properties of hydrate-bearing sediments.

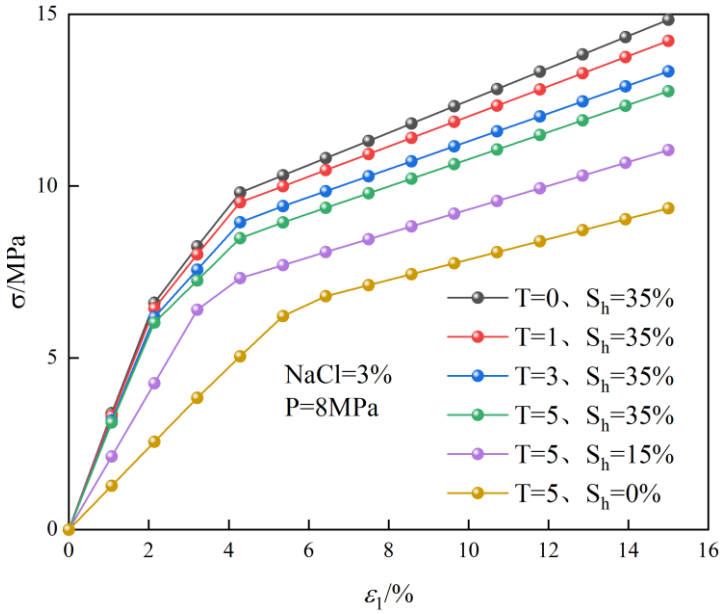

Fig.12 Stress-Strain Curves of the Exploitation Simulation

Analysis of Figures 12 and 13 shows that when no hydrate dissociation occurs (S1-S4), the effect of temperature increase on the mechanical properties of hydrate-bearing sediments is not obvious, and the constitutive relationships in the plastic stage are almost consistent. The yield strengths are 9.17 MPa, 8.93 MPa, 8.42 MPa, and 7.92 MPa respectively, with a small decrease range between different temperature gradients, and the yield strength difference between the maximum temperature difference is 1.25 MPa. The shear strengths are 14.84 MPa, 14.22 MPa, 13.34 MPa, and 12.76 MPa respectively, and the shear strength difference between the maximum temperature difference is 2.08 MPa. Compared with the above-mentioned environmental conditions with a confining pressure of 8 MPa but a temperature below 0°C, the temperature difference has a greater influence on the yield strength and a smaller influence on the shear strength. That is, the relationship between yield strength and temperature is not a simple linear relationship. Therefore, during the exploitation process, with changes in temperature, the settlement of hydrate-bearing sediment reservoirs should be prioritized. When hydrate dissociation occurs (S4-S6), its influence on the mechanical properties of hydrate-bearing sediments is significantly different from that of temperature. The entire stress-strain curves between the three groups of data are quite different, and the slopes in the plastic stage vary greatly. The yield strengths are 7.92 MPa, 7.10 MPa, and 6.49 MPa respectively, and

ISSN: 1813-4890

the yield strength difference between the maximum saturation difference is 1.43 MPa, which is very close to the yield strength difference of 1.49 MPa between the maximum saturation difference under the condition of 8 MPa confining pressure mentioned above. The shear strengths are 12.76 MPa, 11.04 MPa, and 9.35 MPa respectively, and the shear strength difference between the maximum saturation difference is 3.25 MPa, which is slightly smaller than the shear strength difference of 4.2 MPa between the maximum saturation difference under the condition of 8 MPa confining pressure mentioned above. That is, the influence of saturation on hydrate-bearing sediments has a strong linear relationship, but its influence on the mechanical properties of hydrate-bearing sediments is relatively large. Therefore, during the exploitation process, close attention should be paid to hydrate dissociation, and the exploitation can be carried out in stages. After the first exploitation, the hydrate-bearing sediment reservoir can be consolidated for a period of time before the next exploitation.

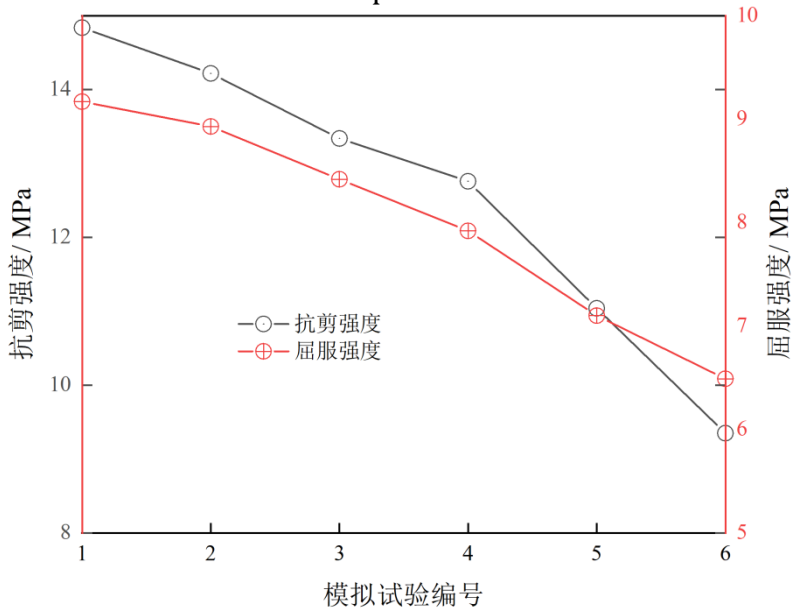

Fig.13 Changes in Yield Strength and Shear Strength

6. Conclusions

In this study, the UHARD subroutine was used to customize the constitutive model of user-defined materials, and the user subroutine interface was utilized to realize the numerical simulation of the evolution laws of the mechanical properties of hydrate-bearing sediments under complex conditions. The triaxial test data under different NaCl concentrations, different temperatures, different hydrate saturations, and different effective confining pressures were compared with the numerical simulation results, and supplementary simulation tests were conducted to analyze the influence of multi-field changes on the mechanical properties of hydrate-bearing sediments. The comparison results show that:

1.The numerical model has a small error and can well reflect the evolution laws of the mechanical properties of hydrate-bearing sediments under complex conditions;

2.The model error is generally caused by the stage with strong non-linearity. When the stress-strain curve has strong non-linearity, the simulation curve will produce slight errors in the transition stage from elastic strain to plastic strain, which does not affect the overall simulation results; when the stress-strain curve is relatively smooth, the simulation effect is good;

3.The relationship between yield strength and temperature is not a simple linear relationship. Therefore, during the exploitation process, with changes in temperature, the settlement of hydrate-bearing sediment reservoirs should be prioritized; hydrate saturation has a significant

impact on mechanical properties, so close attention should be paid to hydrate dissociation during the exploitation process;

4.During the simulation process, it was found that the UHARD customized constitutive model can well meet the user's needs. Through debugging, it was found that UHARD can well reflect the evolution laws of the plastic stage in the stress-strain curve, with simple programming and small calculation load. Therefore, UHARD can be used to realize other research test behaviors of hydrate-bearing sediments; in addition, UHARD can also be used in combination with USDFLD. By using USDFLD to redefine the values of field variables transmitted to UHARD at each material point of the element, the numerical model of hydrate-bearing sediments can be applied more flexibly.

References

[1] ZHOU Shouwei, ZHU Junlong, LI Qingping, et al. Scientifically and steadily achieving the "dual carbon" goal and actively promoting the construction of an energy power [J]. Natural Gas Industry, 2022, 42(12): 1-11.

[2] JIANG Mingjing. New ideas for green, efficient and safe exploitation of hydrates in the Qiongdongnan Sea [J/OL]. Chinese Journal of Geotechnical Engineering, 1-16 [2025-03-13].

[3] DONG Baocan. Numerical simulation study on heat-fluid-solid multi-field coupling and reservoir sand production during natural gas hydrate exploitation [D]. China University of Petroleum (Beijing), 2023.

[4] UCHIDA S, SOGA K, YAMAMOTO K. Critical state soil constitutive model for methane hydrate soil [J]. Journal of Geophysical Research: Solid Earth, 2012, 117(B3): B03209.

[5] Abaqus Scripting User's Manual [M]. Version 6.10. USA, Rhode Island: ABAQUS, Inc., 2010.

[6] WANG Yingyu. Abaqus Analysis User Manual - Material Volume [M]. Beijing: China Machine Press, 2018.

[7] Development and Application of Finite Element Subroutines Based on ABAQUS [M]. (In Chinese)

[8] BARBERO J E. Finite Element Analysis of Composite Materials Using Abaqus® [M]. Taylor and Francis, 2013.

[9] JIN J, ZHANG Y, WEN X, et al. Experimental study of mechanical properties of deep-sea hydrate-bearing sediments under multi-field coupling conditions [J]. Energy Reports, 2024, 10: 2232-2243.

[10] LIU Lin, YAO Yangping, ZHANG Xuhui, et al. Elastoplastic constitutive model for hydrate-bearing sediments [J]. Chinese Journal of Theoretical and Applied Mechanics, 2020, 52(02): 556-566.

[11] YONEDA J, MASUI A, KONNO Y, et al. Mechanical behavior of hydrate-bearing pressure-core sediments visualized under triaxial compression [J]. Marine and Petroleum Geology, 2015, 66: 451-459.

[12] ARORA R, ACHARYA A. A unification of finite deformation J2 Von-Mises plasticity and quantitative dislocation mechanics [J]. Journal of the Mechanics and Physics of Solids, 2020, 143: 104134.

[13] Xiaokun H ,Shengwen Q ,Xiaolin H , et al.Hydrate morphology and mechanical behavior of hydrate-bearing sediments: a critical review[J].Geomechanics and Geophysics for Geo-Energy and Geo-Resources,2022,8(5).